BJR

Received: 17 September 2015 | Revised: 18 November 2015 | Accepted: 25 November 2015

doi: 10.1259/bjr.20150766

Cite this article as:
Zhang F, Yang L, Song X, Li Y-N, Jiang Y, Zhang X-H, et al. Feasibility study of low tube voltage (80 kVp) coronary CT angiography combined with contrast medium reduction using iterative model reconstruction (IMR) on standard BMI patients. *Br J Radiol* 2016; **89**: 20150766.

FULL PAPER

Feasibility study of low tube voltage (80 kVp) coronary CT angiography combined with contrast medium reduction using iterative model reconstruction (IMR) on standard BMI patients

[1]FAN ZHANG, MD, [2]LI YANG, MD, [2]XIANG SONG, MS, [2]YING-NA LI, MS, [3]YAN JIANG, MD, [2]XING-HUA ZHANG, MD, [2]HAI-YUE JU, MD, [2]JIAN WU, MD and [2]RUI-PING CHANG, MS

[1]Department of Radiology, Hainan Branch of Chinese People's Liberation Army General Hospital, Sanya, China
[2]Department of Radiology, Chinese People's Liberation Army General Hospital, Beijing, China
[3]Clinical Science Imaging System, Philips Healthcare, Shanghai, China

Address correspondence to: Dr Li Yang
E-mail: *yli301@163.com*

Objective: To investigate the feasibility of low-tube-voltage (80 kVp) coronary CT angiography (CCTA) combined with contrast medium (CM) reduction and iterative model reconstruction (IMR) on patients with standard body mass index compared with clinical routine protocol.
Methods: Retrospectively gated helical CCTA scans were acquired using a 256-slice multi-slice CT (Brilliance iCT; Philips Healthcare, Cleveland, OH) on 94 patients with standard body mass index (20–25 kg m^{-2}) who were randomly assigned into 2 groups. The scan protocol for Group 1 was 100 kVp and 600 mAs with 70 ml CM at an injection rate of 4.5–5.5 ml s^{-1}; images were reconstructed by a hybrid iterative reconstruction technique (iDose^4; Philips Healthcare). Group 2 was scanned at 80 kVp and 600 mAs with 35 ml CM at an injection rate of 3.5–4.5 ml s^{-1}; images were reconstructed with IMR. Objective measurements such as the mean image noise and contrast-to-noise ratio of the two groups were measured on CT images and compared using the paired t-test. In addition, a subjective image quality evaluation was performed by two radiologists who were blinded to the scan protocol, using a 5-point scale [1 (poor) to 5 (excellent)]. The results of the two groups were compared using Mann–Whitney *U* test.
Results: The iodine delivery rate of Group 2 was 1.0 ± 0.5 gI s^{-1} compared with 2.1 ± 0.5 gI s^{-1} in Group 1 resulting in a reduction of 52.4%. In addition, an effective radiation dose reduction of 56.4% was achieved in Group 2 (2.4 ± 1.2 mSv) compared with Group 1 (5.5 ± 1.4 mSv). The mean CT attenuation, contrast-to-noise ratio and image quality of all segments in Group 2 were significantly improved compared with those in Group 1 (all, $p < 0.01$).
Conclusion: The use of IMR along with a low tube voltage (80 kVp) combined with a low CM protocol for CCTA can reduce both radiation and CM dose with improved image quality.
Advances in knowledge: In this study, we used a novel knowledge-based IMR which remarkably reduced the image noise. We compared the quality of the images obtained when the tube voltage was reduced to 80 kVp and that of those obtained according to the clinical routine protocols to determine whether ultra-low-dose imaging plus IMR is feasible in CCTA scans. We found that a low dose protocol combined with 80 kVp and reduced CM for CCTA can reduce both radiation dose and CM dose with improved image quality by the use of IMR in non-obese patients.

INTRODUCTION

With the development of multidetector CT, coronary CT angiography (CCTA) has become a preferred non-invasive approach to evaluate coronary artery disease,[1,2] but has persistently contributed to a certain burden of radiation dose.[3] Moreover, the use of iodinated contrast medium (CM) for CCTA also remains a concern since it may contribute to renal impairment.[4] Therefore, it is important to find an approach that can optimize both radiation and CM dose in CCTA examinations. Low tube voltage has been investigated as a means to decrease radiation dose as well as to optimize CM dose. The mean photon energy at low tube voltage approaches the iodine K-edge of 33 keV,[5,6] which will result in higher iodine contrast enhancement. However, low tube voltage may also deteriorate the diagnostic quality of CT images by increasing image noise

and/or beam-hardening artefacts. One solution for improving image quality at low tube voltage is to increase tube current to balance image noise;[6] however, this may come at the cost of increased radiation dose, especially on larger patients. Another solution is the use of iterative reconstruction (IR) techniques to address the increased image noise.

During the past decade, IR algorithms were introduced to help reduce the quantum noise associated with standard-convolution filtered back projection (FBP) reconstruction algorithms. Hybrid-type IR (HIR) algorithms have been applied in CCTA in clinical settings, with low-dose acquisitions combined with HIR facilitating dose reductions of up to 63% depending on the proportion of iteration blending with FBP.[7–10] Recently, a knowledge-based iterative algorithm known as iterative model reconstruction (IMR), which represents the latest advances in the field of reconstruction techniques, has been introduced to enable further dose reduction and image quality improvements in low-dose CCTA.[11–14] Previous studies[12,14] demonstrated that IMR yielded significant improvement in both qualitative and quantitative image quality compared with FBP and HIR when using low tube voltage at 100 kVp, indicating a potential for further dose reduction.

Thus, we investigated a dose-saving protocol combining a low tube voltage (80 kVp) and reduced CM along with the use of IMR by comparing the image quality of scans acquired with this protocol with those acquired with a routine clinical protocol reconstructed with HIR to determine whether the new protocol can result in CCTA scans with improved image quality.

METHODS AND MATERIALS

This prospective study received institutional review board approval; prior informed consent was obtained from all patients.

Study population

We prospectively enrolled 94 consecutive patients (44 males and 50 females; mean age 66 ± 13 years) who underwent retrospective helical electrocardiogram (ECG)-gated CCTA between April and August 2013. All had suspected or confirmed coronary artery disease and were referred for CCTA for clinical reasons based on guidelines promulgated by the American College of Cardiology.[15] The inclusion criteria were a body mass index (BMI) between 20 and 25 and an Agatston score <400 Agatston units. Exclusion criteria included the presence of severe arrhythmia, atrial fibrillation, prior coronary artery bypass grafting, heart rate >80 beats per minute (bpm) despite therapy by β-Blocker, allergy to CM, renal insufficiency (estimated glomerular filtration rate $<40\ \mathrm{ml\ min^{-1}\ 1.73\ m^{-2}}$), unstable clinical condition and inability to perform a breath hold.

CT acquisition

We used a 256-slice CT scanner (Brilliance iCT; Philips Healthcare, Cleveland, OH). All CCTA examinations started with a calcium scan without contrast, which produced a coronary artery calcium score following the Agatston method.[16] Thereafter, CCTA scans were performed using retrospective ECG-gated protocol using the following parameters: detector collimation, 128 × 0.625 mm; slice thickness, 0.9 mm; section increment, 0.45 mm; gantry rotation time, 0.27 s; pitch, 0.16; tube current time product, 600 mAs with ECG-dependent tube current modulation; and tube voltage of 100 and 80 kVp for Group 1 and Group 2, respectively. All patients received intravenous contrast (Ultravist® 370; Schering, Berlin, Germany) via an 18-gauge catheter placed in the antecubital vein followed by saline. The injection protocol for Group 1 delivered 70 ml of contrast at 4.5–5.5 $\mathrm{ml\ s^{-1}}$ followed by a saline chaser of 20–30 ml injected at the same rate as the contrast, while the protocol for Group 2 delivered 35 ml of contrast at 3.5–4.5 $\mathrm{ml\ s^{-1}}$ by a saline chaser of 20–30 ml injected at the same rate as the contrast. The start time of data acquisition was determined with a computer-assisted bolus-tracking program (Bolus Tracking; Philips Healthcare) with a trigger threshold of 120 HU in the ascending aorta. Data acquisition started 5 s after triggering. To minimize the presence of motion artefact in our studies, patients with a baseline heart rate of over 75 bpm were treated with intravenous atenolol (5–10 mg) approximately 2–5 min before the scan.

Image reconstruction

The raw data from Group 1 were reconstructed with an HIR algorithm (iDose[4]; Philips Healthcare), and the raw data from Group 2 were reconstructed with a prototype implementation of the new knowledge-based IR algorithm (IMR). All raw data were reconstructed using identical parameters of 0.9 mm thickness at 0.45 mm increment, 512 × 512 pixel matrix, 250 mm field of view (FOV) and a standard cardiac reconstruction kernel (XCB). For Group 1, we applied a moderate-level HIR reconstruction (iDose[4]; Philips Healthcare Level 4) which is routinely used at our hospital. For the IR employed in Group 2, there are two IMR cardiac settings (Cardiac Routine and Cardiac Sharp) each with three levels (L1, L2, and L3). For our reconstructions, we targeted the lowest noise reduction, Level 1, with the cardiac routine setting.

CT radiation dose and iodine delivery rate

Machine-generated CT dose index volume (CTDIvol), scan length, dose-length product (DLP) values and injection rate were recorded for each patient. Estimated effective dose was calculated from the product of DLP and a conversion factor k for the chest ($k = 0.028\ \mathrm{mSv \times mGy^{-1} \times cm^{-1}}$).[17] In order to compare with previous studies focusing on radiation dose of cardiac CT, we performed the effective dose calculation with the old chest conversion factor of 0.014[18] as well.

The iodine load was calculated as contrast concentration multiplied by the total amount of CM, and the iodine delivery rate was calculated as the iodine load multiplied by injection rate.[19]

Image assessment

All images were reviewed and interpreted on a commercially available workstation (Extended Brilliance Workspace v. 4.5.2; Philips Healthcare). Two radiologists with 2 years' experience in CCTA performed objective quantitative assessments on axial source images and recorded the following findings: (1) mean CT attenuation of the proximal, medial and distal segments of the right coronary artery (RCA), left anterior descending (LAD) and left circumflex artery (LCX). For these measurements, a circular region of interest was placed in an area of the vessels that was

not so small as to be affected by pixel variability and not so large as to approach the edges of the vessel. (2) Contrast enhancement of the proximal, medial and distal segments of the RCA, LAD and LCX, calculated as the difference between the mean attenuation in the lumen of the contrast-enhanced vessel and left ventricle. (3) Image noise, determined as the standard deviation of the attenuation value in a single circular region of interest placed in the left ventricle. (4) Contrast-to-noise ratio (CNR) of the proximal, medial and distal segments of the RCA, LAD and LCX, calculated as CNR = contrast enhancement/image noise. We compared these parameters between two groups. The coronary segmentation was according to Society of Cardiovascular CT guidelines for the interpretation and reporting of coronary CT angiography.[20]

For subjective image quality assessment, available images included transverse source images, multiplanar reformations and thin-slab (3 mm) maximum intensity projections. Two cardiovascular radiologists with 5 and 10 years' experience in CCTA, who were blinded to the scan conditions and reconstruction settings, independently evaluated the image quality of the proximal, medial and distal segments of the coronary arteries using a 5-point scale in which 5 (excellent) = images neither noisy nor artifactual, contours smooth and clear, useful diagnostic information; 4 (good) = image slightly noisy or artifactual, clear contours, sufficient diagnostic information; 3 (fair) = image noisy and artifactual, contour partially obscured, acceptable diagnostic information; 2 (poor) = image very noisy and artifactual, insufficient information for diagnosis; and 1 (unacceptable) = severe noise and artefacts, image non-assessable. When they disagreed, a third cardiovascular radiologist with >15 years' experience was asked to adjudicate the differences in order to obtain a consensus score.

Statistical analysis

All continuous values were expressed as mean ± standard deviation. To compare the invariable relationships of the patient demographic and pathological characteristics between groups, we used χ^2 or Fisher's exact test when the predictor was categorical and used Wilcoxon rank sum test when the predictor was quantitative. Differences in the mean values of the objective image quality parameters with normally and non-normally distributed data were determined with the analysis of independent t test and Mann–Whitney U test, respectively. The subjective scores were compared by using the Mann–Whitney U test. Interobserver agreement for subjective image scores was measured using Kappa test. All statistical analyses were performed with commercially available software (SPSS® v. 18.0; IBM Corporation, Armonk, NY; formerly SPSS Inc., Chicago, IL). Two-sided testing was used. A value of $p < 0.05$ was considered to be a statistically significant difference.

RESULTS

Patient demographics and radiation dose

The results of patient demographics are summarized in Table 1. There was no significant difference between the two groups with respect to age, gender, body weight, BMI and the clinical characteristics including hyperlipidemia, hypertension, diabetes mellitus and heart rate.

Radiation dose and iodine delivery rate

The results of radiation dose and iodine delivery rate are summarized in Table 2. In Group 2 and Group 1, the mean CT dose index volume, scan length, DLP, effective radiation dose, injection rate, iodine load and iodine delivery rate were 23.6 ± 2.2 and 11.5 ± 1.2 mGy; 141 ± 15 and 140 ± 17 mm; 392 ± 119 and 169 ± 6 mGy cm; 10.9 ± 2.8/5.5 ± 1.4 and 4.8 ± 2.4/2.4 ± 1.2 mSv; 4.9 ± 0.5 and 3.8 ± 0.6 ml s^{-1}; 0.44 ± 0.05 and 0.26 ± 0.04 gI ml^{-1}; and 2.1 ± 0.5 and 1.0 ± 0.5 gI s^{-1}, respectively. There were significant differences between the two groups for all parameters except scan length. The effective radiation dose and the iodine delivery rate of Group 2 were reduced by 56.4% and 52.4%, respectively, compared with Group 1.

Table 1. Patient demographics

Characteristics	Values		p-value
	Group 1	Group 2	
Age, years, mean ± SD (range)	65 ± 13 (48–82)	68 ± 15 (45–78)	NSD
Male/female, n/n	25/22	19/28	NSD
Body weight, kg, mean ± SD	58.3 ± 7.2	55.7 ± 8.4	NSD
Body mass index, kg m^{-2}, mean ± SD	22.6 ± 2.3	22.4 ± 2.1	NSD
Chest pain, n/N	24/47	28/47	NSD
Hyperlipidemia, n/N (%)	11/47 (23)	9/47 (19)	NSD
Hypertension, n/N (%)	21/47 (45)	18/47 (38)	NSD
Diabetes mellitus, n/N (%)	8/47 (17)	14/47 (30)	NSD
Heart rate, bpm, mean ± SD	62 ± 8	60 ± 9	NSD
Current smoking, n/N (%)	11/47 (23)	15/47 (32)	NSD
Prior smoking, n/N (%)	13/47 (28)	18/47 (38)	NSD

NSD, no significant difference; SD, standard deviation.

Table 2. Radiation dose and iodine delivery rate

Group	Group 1	Group 2	*p*-value
$CTDI_{vol}$ (mGy)	23.6 ± 2.2	11.5 ± 1.2	<0.01
Scan length (mm)	141 ± 15	140 ± 17	NSD
DLP ± SD (mGy cm)	392 ± 119	169 ± 6	<0.01
Effective dose (mSv)			
$k = 0.028$	10.9 ± 2.8	4.8 ± 2.4	<0.01
$k = 0.014$	5.5 ± 1.4	2.4 ± 1.2	<0.01
Injection rate ($ml\,s^{-1}$)	3.8 ± 0.6	4.9 ± 0.5	<0.01
Iodine load ($gI\,ml^{-1}$)	0.44 ± 0.05	0.26 ± 0.04	<0.01
Iodine delivery rate ($gI\,s^{-1}$)	1.8 ± 0.5	1.4 ± 0.5	<0.01

$CTDI_{vol}$, CT dose index volume; DLP, dose-length product; Group 1, 100 kV; Group 2, 80 kV; NSD, no significant difference; SD, standard deviation.

Quantitative analysis

Table 3 and Figure 1 show the results of our quantitative analysis. Both mean CT attenuation and CNR of all segments of LAD, LCX and RCA were significantly greater on Group 2 compared with those of Group 1. The mean CT attenuation and CNR of distal segments of LAD, LCX and RCA in both groups were significantly lower than their corresponding proximal and mid segments. The mean image noise of Group 2 was significantly lower than that of Group 1 (11.5 ± 3.8 HU and 27.1 ± 5.3 HU, respectively, $p = 0.024$).

Qualitative results

Table 4 summarizes the kappa value and the subjective image quality scores of the LAD, LCX and RCA for the two reviewers. The two radiologists showed very good consistency in qualitative assessment, kappa value = 0.46–0.78. A significant difference was found between Group 1 and Group 2 for image quality scores of proximal, mid and distal segments of LAD, LCX and RCA. Group 2 (80 kVp with IMR) scoring was significantly better than Group 1 (100 kVp with HIR). Moreover, the subjective rankings of proximal segments of LAD, LCX and RCA were significantly higher than their corresponding mid and distal segments in Group 1; in contrast, there were no significant differences in image quality scores among segments in Group 2. Representative cases are shown in Figures 2–4.

DISCUSSION

To our knowledge, this study is the first clinical study of IMR with combined low tube voltage (80 kVp) and low CM protocol in CCTA. Previous studies[21,22] demonstrated that the use of a low tube voltage protocol at 100 kVp could facilitate significant reduction of radiation exposure in non-obese patients while at the same time maintaining image quality compared with a 120 kVp protocol in CCTA. Moreover, other studies[7,23–25] demonstrated that the use of HIR techniques enabled improvement to image quality of CCTA in low-dose protocols. Thus, 100 kVp plus HIR protocols are supposed to be at least as good or better when compared with 120 kVp employing FBP on patients with standard BMI. Therefore, we adopted the protocol of 100 kVp plus HIR as clinical routine in our institute and as the control group in this study. For the experimental group, we proposed a combined dose-saving protocol using 80 kVp with both reduced volume and injection rate of CM. In theory, the use of 80 kVp enables further radiation dose reduction[26] and improved enhancement of vascular structures when compared with 100 kVp.[5,6] However, reduced contrast volume and injection rate may lead to insufficient peak intravascular enhancement and thus adversely impact the image quality of CCTA scans.[27] Our results demonstrated that the use of 80 kVp not only reduced the radiation dose by about half in Group 2, but also increased the mean CT attenuation of all coronary segments in this group compared with those in Group 1, despite the reduction of CM (in Group 2). This demonstrates that 80 kVp could effectively compensate for reduced CM owing to its X-ray output approaching the K-edge of iodine. The reduction of CM is especially helpful for patients with renal dysfunction since contrast-induced nephropathy is closely related to pre-existing renal insufficiency and the amount of contrast injected.[4,28] In addition, high flow rate may sometimes be associated with a higher extravasation rate.[29] Thus, the combined dose-saving protocol can be helpful to minimize diagnostically appropriate amount of CM to help reduce the incidence of contrast-induced nephropathy and other adverse reaction.

On the other hand, the use of IMR in Group 2 resulted in a significant decrease in image noise at 80 kVp. IMR is an advanced IR algorithm that uses a knowledge-based approach to accurately determine the data, image statistics and system models of CT scanner and produces optimal images by iteratively minimizing the difference between acquired data and their ideal form.[14] In theory, image noise can be removed during IMR reconstruction, resulting in an artefact- and noise-free image. Similar to previous studies,[12,14] our results showed that IMR yielded significant noise reductions at low tube voltage and helped to improve CNR and image quality. However, excessive image noise reduction could result in image blurring and resolution degradation, with early studies[8,30,31] suggesting that some implementations of iterative approaches could produce images that are significantly different in

Table 3. Mean CT attenuation value and mean contrast-to-noise ratio of the proximal, medial and distal vessels

Objective parameters	LAD			LCX			RCA		
	Proximal	Mid	Distal	Proximal	Mid	Distal	Proximal	Mid	Distal
CT attenuation									
Group 1	468.8 ± 10.3	445.6 ± 14.1	430.1 ± 11.9[a,b]	458.4 ± 14.3	423.9 ± 15.5[a]	448.3 ± 14.9[a,b]	476.3 ± 15.3	472.4 ± 13.8	448.3 ± 14.9[a,b]
Group 2	572.8 ± 14.7	570.3 ± 18.2	532.16 ± 14.7[a,b]	575.2 ± 17.2	524.7 ± 15.1[a]	549.6 ± 15.2[a,b]	566.9 ± 14.8	569.2 ± 15.0	549.6 ± 15.2[a,b]
p-value	<0.01	<0.01	<0.01	<0.01	<0.01	<0.01	<0.01	<0.01	<0.01
Contrast-to-noise ratio									
Group 1	13.8 ± 1.6	12.9 ± 1.3	12.1 ± 1.2[a,b]	13.3 ± 1.6	11.8 ± 1.5[a]	12.8 ± 1.6[a,b]	13.8 ± 1.3	13.6 ± 1.5	12.8 ± 1.6[a,b]
Group 2	44.9 ± 2.3	42.8 ± 2.5	41.9 ± 2.5[a,b]	45.6 ± 2.5	41.6 ± 2.3[a]	40.2 ± 2.1[a,b]	42.2 ± 2.1	41.8 ± 2.4	40.2 ± 2.1[a,b]
p-value	<0.01	<0.01	<0.01	<0.01	<0.01	<0.01	<0.01	<0.01	<0.01

Group 1, 100 kVp; Group 2, 80 kVp; LAD, left anterior descending artery; LCX, left circumflex artery; RCA, right coronary artery.
[a]Significant difference compared with proximal vessel.
[b]Significant difference compared with mid vessel.

Figure 1. Box plot shows the results of quantitative analysis of image noise. Image noise was significantly different between the two groups. Group 1, 100 kVp, hybrid-type iterative reconstruction (HIR); Group 2, 80 kVp, iterative model reconstruction (IMR). HU, Hounsfield unit.

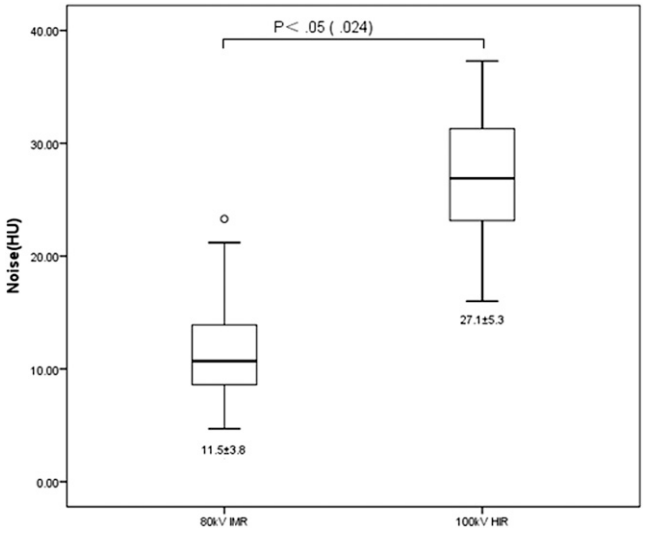

appearance compared with images reconstructed with FBP, with the noise removal manifesting as an "unnatural" over-smoothing of the image. More recent HIR techniques overcome these issues to some degree by reducing noise uniformly across all frequency ranges and yield a more natural image appearance.[25,32] In our study, both HIR and IMR yielded images with a more natural appearance, with the results of Group 2 indicating that IMR enabled similar or superior spatial resolution at low dose compared with HIR. Our findings are consistent with two phantom studies which were performed using abdomen and head scan parameters.[33,34] However, knowledge-based IR such as IMR are non-linear and the spatial resolution obtained varies with the object contrast and noise level; hence, qualitative or semi-quantitative approaches may be more appropriate for meaningful image quality assessments when IMR is employed. In addition, IMR exhibited improved image quality of mid and distal vessel segments in this study, which was also observed by Halpern et al[13] and Oda et al.[14] Furthermore, while we found a significant reduction of image quality scores in mid and distal segments of the images in Group 1 (100 kV with HIR) compared with their proximal segments, no such difference of image quality scores was found among segments in Group 2 (80 kVp with IMR), which indicated that 80 kVp combined with IMR may have additional advantages in improving the overall image quality. We attribute this observation primarily to the improvement in low- and high-contrast detectabilities that are facilitated by IMR in reducing image noise and artefacts and the use of 80 kVp protocols enhancing the vascular structures.

Our study was performed on patients with standard BMI and Agatston scores <400 because low tube voltage protocols were considered not suitable for patients with high BMI and/or severe

Table 4. Qualitative analysis of each reviewer

Readers	LAD			LCX		RCA		
	Proximal	Mid	Distal	Proximal	Distal	Proximal	Mid	Distal
Image quality score								
R-1								
Group 1	3.5 ± 0.5[a]	3.3 ± 0.5[a]	3.2 ± 0.5	3.4 ± 0.5	3.3 ± 0.5	3.5 ± 0.5	3.3 ± 0.4[a]	3.1 ± 0.4[a,b]
Group 2	3.9 ± 0.5	3.8 ± 0.4	3.8 ± 0.5	3.9 ± 0.4	3.7 ± 0.4[a]	3.9 ± 0.4	3.8 ± 0.4	3.8 ± 0.5
R-2								
Group 1	3.6 ± 0.5[a]	3.2 ± 0.5[a]	3.2 ± 0.4	3.3 ± 0.4	3.2 ± 0.6	3.3 ± 0.2	3.2 ± 0.5	3.1 ± 0.4[a]
Group 2	3.9 ± 0.4	3.9 ± 0.3	3.8 ± 0.4	3.9 ± 0.4	3.8 ± 0.4	3.9 ± 0.4	3.9 ± 0.4	3.8 ± 0.4
Final								
Group 1	3.5 ± 0.5	3.2 ± 0.5[a]	3.2 ± 0.4[a]	3.3 ± 0.4	3.2 ± 0.6[a]	3.3 ± 0.2	3.2 ± 0.5[a]	3.1 ± 0.4[a]
Group 2	3.9 ± 0.4	3.8 ± 0.4	3.8 ± 0.4	3.9 ± 0.4	3.7 ± 0.4	3.9 ± 0.4	3.8 ± 0.4	3.8 ± 0.4
p- value	< 0.01	< 0.01	< 0.01	< 0.01	< 0.01	< 0.01	< 0.01	< 0.01
Kappa value								
Group 1	0.67	0.62	0.70	0.65	0.65	0.46	0.67	0.78
Group 2	0.71	0.68	0.71	0.78	0.70	0.78	0.68	0.72

Group 1, 100 kVp; Group 2, 80 kVp; LAD, left anterior descending artery; LCX, left circumflex artery; R-1, Reader 1; R-2, Reader 2; RCA, right coronary artery.
[a]Significant difference compared with proximal vessel.
[b]Significant difference compared with mid vessel.

calcified plaques owing to increased image noise and blooming artefacts from dense structures. Nevertheless, our results revealed that IMR was able to yield superior noise reduction at 80 kVp in non-obese patients which may be further extended to larger patients. Meanwhile, Oda et al[11] reported that IMR was able to reduce artefacts that may help to improve visual evaluation of coronary plaques, while den Harder et al[35] observed that Agatston scores were decreased significantly when using IMR; thus, we suggest further investigations with a gold standard to be performed to assess the accuracy of IMR in severe calcified plaques.

Our study has several limitations. Foremost, the diagnostic performance of our observers in the detection of coronary stenosis was not evaluated because the prevalence of lesions in this study was too low and we had no reference standard for the majority of lesions. Consequently, future studies are needed to evaluate the diagnostic performance of coronary stenosis with IMR by correlating imaging findings with the results of coronary catheterization (reference standard). Second, considering prospective ECG-gated technique requires a relatively steady low heart rate and cannot be used to assess cardiac function because the images are acquired at

Figure 2. Axial cardiac CT images of the proximal left anterior descending coronary artery of a 65-year-old male (body mass index, 22) (Group 1) (a) and 63-year-old male (body mass index, 22) (Group 2) (b) with a partially calcified plaque (arrows). Images reconstructed with iterative model reconstruction (IMR) algorithm (b) show lower image noise than those reconstructed with hybrid-type iterative reconstruction (HIR) algorithm (a). The plaque contour is clearly identified with IMR and HIR. A, above; F, front; L, left.

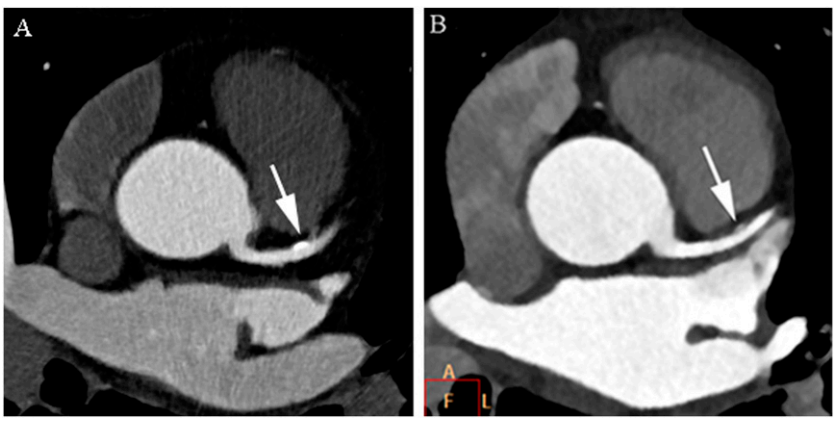

Figure 3. Axial cardiac CT images of the normal distal right coronary artery (arrows) of a 55-year-old male (body mass index, 24) (Group 1) (a) and 58-year-old male (body mass index, 24) (Group 2) (b). Images reconstructed with iterative model reconstruction (IMR) algorithm (b) show lower image noise than those reconstructed with hybrid-type iterative reconstruction (HIR) algorithm (a) (arrowheads).

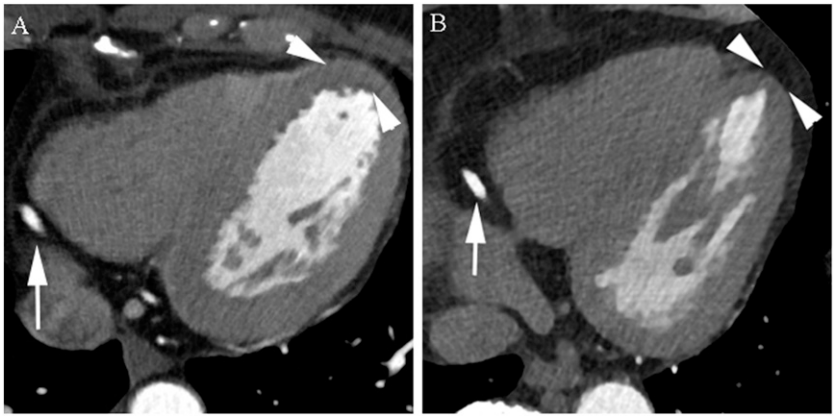

a single, predetermined, end-diastolic, quiescent phase. The retrospective-gated technique is still useful for some patients, and is a protocol where radiation dose reduction is important. Hence, we adopted retrospective-gated CCTA in our investigation. However, the use of prospective ECG-gated techniques could enable further reductions to radiation dose bringing it down into the sub-mSv range. Third, since the appearance of IMR images was significantly different from that of HIR images, it could have potentially influenced the readers and posed a challenge for the double-blinded assessment of subjective image quality, by introducing a bias in the image quality scores. Hence, further exploration such as multiple observer study may help with a better assessment of image quality of the knowledge-based IR.

CONCLUSION

In conclusion, the use of knowledge-based IMR in a dose-saving protocol which combines 80 kVp with reduced CM offers significant reductions in image noise and improvements in image quality. Improvements were measured across all coronary segments compared with the 100 kVp HIR protocol with a standard injection dose for non-obese patients. Radiation dose savings of 56.4% and CM dose savings of 52.4% were achieved by the use of the dose-saving protocol.

FUNDING

This study was supported in part by the Hainan Province of Social Development of Science and Technology Special Projects (number: SF201428) from Hainan Provincial Department

Figure 4. Multiplanar reconstruction cardiac CT images of the right coronary artery of a 62-year-old male (body mass index, 23) (a) and 68-year-old male (body mass index, 24) (b) with a partially non-calcified and calcified plaque. Images reconstructed with iterative model reconstruction (IMR) algorithm (b) show lower image noise than those reconstructed with hybrid-type iterative reconstruction (HIR) algorithm (a). The plaque contour is clearly identified with IMR and HIR algorithms.

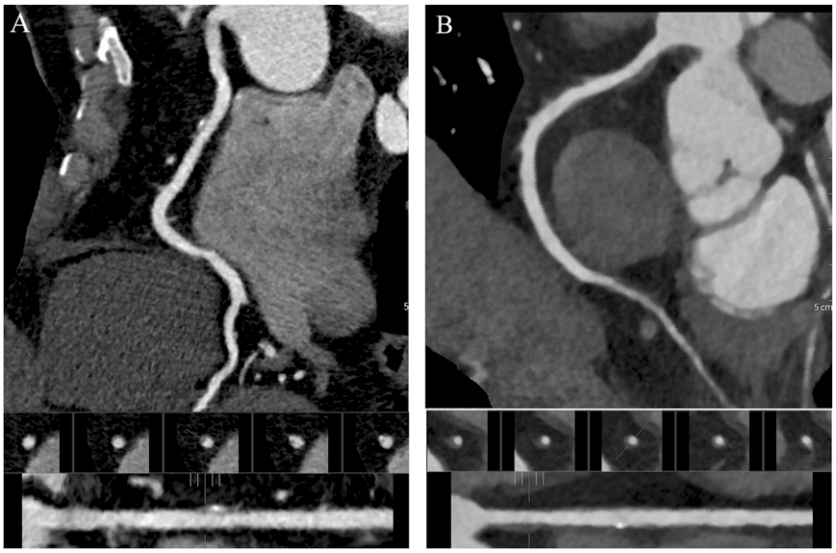

of Science and Technology, Hainan Province, China, and a research grant from (number: 20100481478 to Dr F Zhang) from the China Postdoctoral Science Foundation, Beijing, China.

ACKNOWLEDGMENTS

We thank Mani Vembar, Amar Dhanantwari and Walter Giepmans for their editorial assistance and valuable suggestions about the manuscript.

REFERENCES

1. Mowatt G, Cummins E, Waugh N, Walker S, Cook J, Jia X, et al. Systematic review of the clinical effectiveness and cost-effectiveness of 64-slice or higher computed tomography angiography as an alternative to invasive coronary angiography in the investigation of coronary artery disease. *Health Technol Assess* 2008; **12**: iii–iv, ix–143.
2. Miller JM, Rochitte CE, Dewey M, Arbab-Zadeh A, Niinuma H, Gottlieb I, et al. Diagnostic performance of coronary angiography by 64-row CT. *N Engl J Med* 2008; **359**: 2324–36. doi: 10.1056/NEJMoa0806576
3. Sabarudin A, Sun Z, Ng KH. A systematic review of radiation dose associated with different generations of multidetector CT coronary angiography. *J Med Imaging Radiat Oncol* 2012; **56**: 5–17. doi: 10.1111/j.1754-9485.2011.02335.x
4. Ardekani MS, Issa M, Green L. Diagnostic and economic impact of heart failure induced mediastinal lymphadenopathy. *Int J Cardiol* 2006; **109**: 137–8. doi: 10.1016/j.ijcard.2005.04.011
5. Bae KT. Intravenous contrast medium administration and scan timing at CT: considerations and approaches. *Radiology* 2010; **256**: 32–61. doi: 10.1148/radiol.10090908
6. Nakaura T, Awai K, Maruyama N, Takata N, Yoshinaka I, Harada K, et al. Abdominal dynamic CT in patients with renal dysfunction: contrast agent dose reduction with low tube voltage and high tube current-time product settings at 256-detector row CT. *Radiology* 2011; **261**: 467–76. doi: 10.1148/radiol.11110021
7. Hou Y, Liu X, Xv S, Guo W, Guo Q. Comparisons of image quality and radiation dose between iterative reconstruction and filtered back projection reconstruction algorithms in 256-MDCT coronary angiography. *AJR Am J Roentgenol* 2012; **199**: 588–94. doi: 10.2214/AJR.11.7557
8. Leipsic J, Labounty TM, Heilbron B, Min JK, Mancini GB, Lin FY, et al. Adaptive statistical iterative reconstruction: assessment of image noise and image quality in coronary CT angiography. *AJR Am J Roentgenol* 2010; **195**: 649–54. doi: 10.2214/AJR.10.4285
9. Kropil P, Bigdeli AH, Nagel HD, Antoch G, Cohnen M. Impact of increasing levels of advanced iterative reconstruction on image quality in low-dose cardiac CT angiography. *Rofo* 2014; **186**: 567–75. doi: 10.1055/s-0033-1356074
10. Wang R, Schoepf UJ, Wu R, Reddy RP, Zhang C, Yu W, et al. Image quality and radiation dose of low dose coronary CT angiography in obese patients: sinogram affirmed iterative reconstruction versus filtered back projection. *Eur J Radiol* 2012; **81**: 3141–5. doi: 10.1016/j.ejrad.2012.04.012
11. Oda S, Utsunomiya D, Funama Y, Katahira K, Honda K, Tokuyasu S, et al. A knowledge-based iterative model reconstruction algorithm: can super-low-dose cardiac CT be applicable in clinical settings? *Acad Radiol* 2014; **21**: 104–10. doi: 10.1016/j.acra.2013.10.002
12. Yuki H, Utsunomiya D, Funama Y, Tokuyasu S, Namimoto T, Hirai T, et al. Value of knowledge-based iterative model reconstruction in low-kV 256-slice coronary CT angiography. *J Cardiovasc Comput Tomogr* 2014; **8**: 115–23. doi: 10.1016/j.jcct.2013.12.010
13. Halpern EJ, Gingold EL, White H, Read K. Evaluation of coronary artery image quality with knowledge-based iterative model reconstruction. *Acad Radiol* 2014; **21**: 805–11. doi: 10.1016/j.acra.2014.02.017
14. Oda S, Weissman G, Vembar M, Weigold WG. Iterative model reconstruction: improved image quality of low-tube-voltage prospective ECG-gated coronary CT angiography images at 256-slice CT. *Eur J Radiol* 2014; **83**: 1408–15. doi: 10.1016/j.ejrad.2014.04.027
15. Taylor AJ, Cerqueira M, Hodgson JM, Mark D, Min J, O'Gara P, et al. ACCF/SCCT/ACR/AHA/ASE/ASNC/NASCI/SCAI/SCMR 2010 Appropriate Use Criteria for Cardiac Computed Tomography. A Report of the American College of Cardiology Foundation Appropriate Use Criteria Task Force, the Society of Cardiovascular Computed Tomography, the American College of Radiology, the American Heart Association, the American Society of Echocardiography, the American Society of Nuclear Cardiology, the North American Society for Cardiovascular Imaging, the Society for Cardiovascular Angiography and Interventions, and the Society for Cardiovascular Magnetic Resonance. *Circulation* 2010; **122**: e525–55. doi: 10.1161/CIR.0b013e3181fcae66
16. Agatston AS, Janowitz WR, Hildner FJ, Zusmer NR, Viamonte M Jr, Detrano R. Quantification of coronary artery calcium using ultrafast computed tomography. *J Am Coll Cardiol* 1990; **15**: 827–32. doi: 10.1016/0735-1097(90)90282-T
17. Gosling O, Loader R, Venables P, Rowles N, Morgan-Hughes G, Roobottom C. Cardiac CT: are we underestimating the dose? A radiation dose study utilizing the 2007 ICRP tissue weighting factors and a cardiac specific scan volume. *Clin Radiol* 2010; **65**: 1013–17. doi: 10.1016/j.crad.2010.08.001
18. McCollough CH. CT dose: how to measure, how to reduce. *Health Phys* 2008; **95**: 508–17. doi: 10.1097/01.HP.0000326343.35884.03
19. Jo SH, Youn TJ, Koo BK, Park JS, Kang HJ, Cho YS, et al. Renal toxicity evaluation and comparison between visipaque (iodixanol) and hexabrix (ioxaglate) in patients with renal insufficiency undergoing coronary angiography: the RECOVER study: a randomized controlled trial. *J Am Coll Cardiol* 2006; **48**: 924–30. doi: 10.1016/j.jacc.2006.06.047
20. Leipsic J, Abbara S, Achenbach S, Cury R, Earls JP, Mancini GJ, et al. SCCT guidelines for the interpretation and reporting of coronary CT angiography: a report of the Society of Cardiovascular Computed Tomography Guidelines Committee. *J Cardiovasc Comput Tomogr* 2014; **8**: 342–58. doi: 10.1016/j.jcct.2014.07.003
21. Hausleiter J, Martinoff S, Hadamitzky M, Martuscelli E, Pschierer I, Feuchtner GM, et al. Image quality and radiation exposure with a low tube voltage protocol for coronary CT angiography results of the PROTECTION II Trial. *JACC Cardiovasc Imaging* 2010; **3**: 1113–23. doi: 10.1016/j.jcmg.2010.08.016
22. Feuchtner GM, Jodocy D, Klauser A, Haberfellner B, Aglan I, Spoeck A, et al. Radiation dose reduction by using 100-kV tube voltage in cardiac 64-slice computed tomography: a comparative study. *Eur J Radiol* 2010; **75**: e51–6. doi: 10.1016/j.ejrad.2009.07.012
23. Hou Y, Ma Y, Fan W, Wang Y, Yu M, Vembar M, et al. Diagnostic accuracy of low-dose 256-slice multi-detector coronary CT angiography using iterative reconstruction in patients with suspected coronary artery

disease. *Eur Radiol* 2014; **24**: 3–11. doi: 10.1007/s00330-013-2969-9

24. Itatani R, Oda S, Utsunomiya D, Funama Y, Honda K, Katahira K, et al. Reduction in radiation and contrast medium dose via optimization of low-kilovoltage CT protocols using a hybrid iterative reconstruction algorithm at 256-slice body CT: phantom study and clinical correlation. *Clin Radiol* 2013; **68**: e128–35. doi: 10.1016/j.crad.2012.10.014
25. Funama Y, Taguchi K, Utsunomiya D, Oda S, Yanaga Y, Yamashita Y, et al. Combination of a low-tube-voltage technique with hybrid iterative reconstruction (iDose) algorithm at coronary computed tomographic angiography. *J Comput Assist Tomogr* 2011; **35**: 480–5. doi: 10.1097/RCT.0b013e31821fee94
26. Mahesh M, Hevezi JM. Slice wars vs dose wars in multiple-row detector CT. *J Am Coll Radiol* 2009; **6**: 201–2. doi: 10.1016/j.jacr.2008.11.027
27. Lell MM, Jost G, Korporaal JG, Mahnken AH, Flohr TG, Uder M, et al. Optimizing contrast media injection protocols in state-of-the art computed tomographic angiography. *Invest Radiol* 2015; **50**: 161–7. doi: 10.1097/RLI.0000000000000119
28. Buls N, Van Gompel G, Van Cauteren T, Nieboer K, Willekens I, Verfaillie G, et al. Contrast agent and radiation dose reduction in abdominal CT by a combination of low tube voltage and advanced image reconstruction algorithms. *Eur Radiol* 2015; **25**: 1023–31. doi: 10.1007/s00330-014-3510-5
29. Mihl C, Kok M, Wildberger JE, Turek J, Muehlenbruch G, Das M. Computed tomography angiography with high flow rates: an *in vitro* and *in vivo* feasibility study. *Invest Radiol* 2015; **50**: 464–9. doi: 10.1097/RLI.0000000000000153
30. Leipsic J, Labounty TM, Heilbron B, Min JK, Mancini GB, Lin FY, et al. Estimated radiation dose reduction using adaptive statistical iterative reconstruction in coronary CT angiography: the ERASIR study. *AJR Am J Roentgenol* 2010; **195**: 655–60. doi: 10.2214/AJR.10.4288
31. Silva AC, Lawder HJ, Hara A, Kujak J, Pavlicek W. Innovations in CT dose reduction strategy: application of the adaptive statistical iterative reconstruction algorithm. *AJR Am J Roentgenol* 2010; **194**: 191–9. doi: 10.2214/AJR.09.2953
32. Utsunomiya D, Weigold WG, Weissman G, Taylor AJ. Effect of hybrid iterative reconstruction technique on quantitative and qualitative image analysis at 256-slice prospective gating cardiac CT. *Eur Radiol* 2012; **22**: 1287–94. doi: 10.1007/s00330-011-2361-6
33. Suzuki S, Haruyama T, Morita H, Takahashi Y, Matsumoto R. Initial performance evaluation of iterative model reconstruction in abdominal computed tomography. *J Comput Assist Tomogr* 2014; **38**: 408–14. doi: 10.1097/RCT.0000000000000062
34. Löve A, Olsson ML, Siemund R, Stålhammar F, Björkman-Burtscher IM, Söderberg M. Six iterative reconstruction algorithms in brain CT: a phantom study on image quality at different radiation dose levels. *Br J Radiol* 2013; **86**: 20130388. doi: 10.1259/bjr.20130388
35. den Harder AM, Willemink MJ, Bleys RL, de Jong PA, Budde RP, Schilham AM, et al. Dose reduction for coronary calcium scoring with hybrid and model-based iterative reconstruction: an *ex vivo* study. *Int J Cardiovasc Imaging* 2014; **30**: 1125–33. doi: 10.1007/s10554-014-0434-8